JOURNAL OF BACTERIOLOGY, May 1994, p. 2922–2929
0021-9193/94/$04.00+0

Vol. 176, No. 10

Aromatic Amine Dehydrogenase, a Second Tryptophan Tryptophylquinone Enzyme

SHANTHI GOVINDARAJ,[1]† EDWARD EISENSTEIN,[1,2] LIMEI HSU JONES,[3] JOANN SANDERS-LOEHR,[4] ANDREI Y. CHISTOSERDOV,[5] VICTOR L. DAVIDSON,[3] AND STEVEN L. EDWARDS[6]*

Center for Advanced Research in Biotechnology, Rockville, Maryland 20850[1]; Departments of Chemistry and Biochemistry, University of Maryland—Baltimore County, Baltimore, Maryland 21228[2]; Department of Biochemistry, The University of Mississippi Medical Center, Jackson, Mississippi 39216-4505[3]; Department of Chemistry, Biochemistry, and Molecular Biology, Oregon Graduate Institute of Science and Technology, Portland, Oregon 97291-1000[4]; Environmental Engineering Science, W. M. Keck Laboratories, California Institute of Technology, Pasadena, California 91125[5]; and Laboratory of Structural Biology, National Institute of Arthritis and Musculoskeletal and Skin Diseases, Bethesda, Maryland 20892[6]

Received 15 December 1993/Accepted 12 March 1994

Aromatic amine dehydrogenase (AADH) catalyzes the oxidative deamination of aromatic amines including tyramine and dopamine. AADH is structurally similar to methylamine dehydrogenase (MADH) and possesses the same tryptophan tryptophylquinone (TTQ) prosthetic group. AADH exhibits an $\alpha_2\beta_2$ structure with subunit molecular weights of 39,000 and 18,000 and with a quinone covalently attached to each β subunit. Neither subunit cross-reacted immunologically with antibodies to the corresponding subunits of MADH, and the N-terminal amino acid sequence of the β subunit of AADH exhibited no homology with the highly conserved β subunits of MADH. The absorption spectra for the oxidized, semiquinone, and reduced forms of AADH have been characterized, and extinction coefficients for the absorption maxima of each redox form have been determined. These spectra are very similar to those for MADH, indicating the likelihood of a TTQ cofactor. This was verified by the near identity of the vibrational frequencies and intensities in the resonance Raman spectra for the oxidized forms of AADH and MADH. A stable semiquinone of AADH could be observed during a reductive titration with dithionite, whereas titration with tyramine proceeded directly from the oxidized to the reduced form. AADH was very stable against denaturation by heat and exposure to guanidine. The individual subunits could be separated by gel filtration after incubation in guanidine hydrochloride, and partial reconstitution of activity was observed on recombination of the subunits. Steady-state kinetic analysis of AADH yielded a V_{max} of 17 μmol/min/mg and a K_m for tyramine of 5.4 μM. Substrate inhibition by tyramine was observed. AADH was irreversibly inhibited by hydrazine, phenylhydrazine, hydroxylamine, semicarbazide, and aminoguanidine. Isonicotinic acid hydrazide (isoniazid) and isonicotinic acid 2-isopropyl hydrazide (iproniazid) were reversible noncompetitive inhibitors of AADH and exhibited K_i values of 8 and 186 μM, respectively. The similarities and differences between AADH and other amine oxidizing enzymes are also discussed.

Alcaligenes faecalis is a gram-negative soil bacterium which can also be a human pathogen. It utilizes organic acids and amino acids in preference to common carbohydrates. It is also able to metabolize certain aromatic amine compounds for use as a carbon source. This class of compounds includes β-phenylethylamines in which the phenyl ring may be hydroxylated, as in tyramine and dopamine. Tyramine, a decarboxylation product of tyrosine, is found in various animals and microorganisms and in putrefied tissue. The catabolism of aromatic amines in many bacteria is initiated by oxidative deamination of the amine by a monoamine oxidase (30). Alternatively, *A. faecalis* performs oxidative deamination of aromatic amines using a dehydrogenase. This enzyme, called aromatic amine dehydrogenase (AADH), was originally isolated and characterized by Iwaki et al. (20). Their efforts yielded a highly purified form of the enzyme and a preliminary determination of its kinetic, spectral, and structural properties. It was noted that AADH contained an unusual green chromophore, which the authors suggested might be a pyrrole-quinone similar to the cofactor then suspected for methylamine dehydrogenase (MADH) (13, 15).

Much effort has been directed towards understanding the structure of MADH and its prosthetic group, which is now known to be tryptophan tryptophylquinone (TTQ) (Fig. 1). TTQ is formed by posttranslational modification of two gene-encoded tryptophan residues (5), which leads to a covalent attachment between the indole rings of the two tryptophan residues and oxidation of one indole ring to an *o*-quinone (26). This structure has been confirmed by X-ray crystallography (3). TTQ in three different MADHs has been analyzed by resonance Raman spectroscopy (1, 25). This has resulted in the assignment of many structural features of the chromophore to specific peaks in the resonance Raman spectrum and the characterization of spectral features which are diagnostic of TTQ.

MADH has been the only known example of a TTQ-bearing enzyme. Resonance Raman studies of AADH in the present work show that it also possesses TTQ as a prosthetic group. In

* Corresponding author. Mailing address: National Institutes of Health, NIAMS, Building 6, Room 425, 9000 Rockville Pike, Bethesda, MD 20892. Phone: (301) 402-3223. Fax: (301) 402-3417.

† Current address: Department of Molecular Biology and Biochemistry, University of California, Irvine, CA.

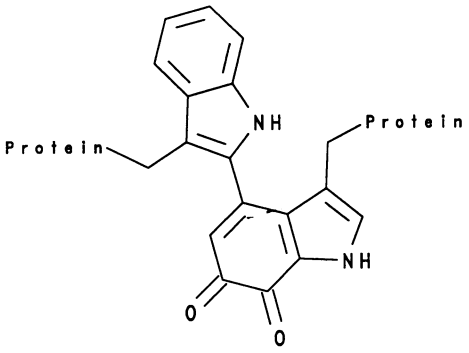

FIG. 1. Structure of TTQ.

addition, this paper presents a detailed analysis of the physical properties and kinetics of AADH for comparison with MADH. We find that the subunit molecular weights and extinction coefficient of AADH differ from those reported previously (20). The correct determination of the properties of AADH and characterization of the similarities and differences between AADH and MADH are important steps in understanding the role of TTQ in enzyme catalysis and electron transfer.

MATERIALS AND METHODS

Materials. *A. faecalis* IFO 14479 was purchased from the Institute for Fermentation in Osaka, Japan. All reagents were purchased from Sigma Chemical Company.

Methods. (i) Bacterial growth. *A. faecalis* was grown in the medium described by Iwaki et al. (20) with 0.15% β-phenylethylamine as a carbon source.

(ii) Protein purification. Cell extracts of *A. faecalis* which were used as a source of AADH were prepared by sonication. Approximately 90 g (wet weight) of cells was processed for the purification, which is described in Table 1. The cell extract was fractionated between 35 and 85% ammonium sulfate. The precipitate from the ammonium sulfate fractionation was dialyzed against 10 mM potassium phosphate, pH 7.5, and applied to a Whatman DE52 cellulose column (25 by 5 cm) which had been equilibrated in the dialysis buffer. The column was eluted with a linear gradient of 0 to 250 mM NaCl in 10 mM potassium phosphate, pH 7.5. Fractions containing AADH eluted at approximately 200 mM NaCl. These fractions were pooled, concentrated by ultrafiltration, and applied to an AcA 34 (Spectrum) gel filtration column (120 by 7.5 cm). The column was eluted with 50 mM potassium phosphate, pH 7.5. Fractions containing the purified protein were pooled, concentrated, and stored frozen in 10% ethylene glycol for future use. Protein concentrations were determined by the method of Bradford (2) with bovine serum albumin as a standard. MADH from *Paracoccus denitrificans* was purified as described previously (8).

(iii) Subunit separation and reconstitution. To effect the complete denaturation of the enzyme, purified AADH was incubated for 48 h at room temperature in 50 mM potassium phosphate buffer, pH 6.9, which contained 6 M guanidine hydrochloride. The subunits were separated by gel filtration on a Sephadex G-100 column equilibrated with 50 mM potassium phosphate buffer, pH 6.9, containing 0.5 M guanidine hydrochloride.

(iv) Enzyme assay. AADH activity was measured by the same method as that used to assay MADH (8) with the exception of the use of tyramine as the substrate amine. Assays were performed with either phenazine methosulfate or phenazine ethosulfate as the immediate electron acceptor.

(v) Spectroscopic techniques. Absorption spectra were recorded with a Milton Roy 3000 diode array spectrophotometer. To achieve anaerobic conditions, the cuvette was connected by a Firestone rapid purge valve (Ace Glass, Vineland, N.J.) to a vacuum pump and a source of oxygen-free argon. By use of the valve, it was possible to alternate cycles of evacuation and flushing of the cuvette with argon. Such cycling was repeated for approximately 25 min prior to each assay, which was performed under an argon atmosphere. Raman spectra were recorded on a Jarrell-Ash 25-300 spectrometer (1). Samples were frozen onto the cold tip of a helium refrigerator (Displex Air Products), maintained at 15 K, and illuminated in a 150° backscattering geometry with a Spectra-Physics 164 argon ion laser.

(vi) Electrophoresis. Sodium dodecyl sulfate-polyacrylamide gel electrophoresis (SDS-PAGE) was performed according to Laemmli (23). The redox-cycling stain for detection of quinoproteins was performed according to Paz et al. (34). Isoelectric focusing was performed in a polyacrylamide gel with a Pharmacia PhastSystem with standard protein markers which ranged from pI 3.5 to 8.6. The gel was run and analyzed according to the instructions of the manufacturer.

(vii) Immunological analysis. Western blots (immunoblots), with alkaline phosphatase-conjugated immunoglobulin G (Promega Biotec, Madison, Wis.) as a second antibody, were performed with Bio-Rad reagents and equipment according to the instructions of the manufacturer.

(viii) Holoenzyme molecular weight determination. Sedimentation equilibrium was performed with a Beckman model E ultracentrifuge essentially as described by Nichols et al. (31). Double-sector cells with charcoal-filled Epon centerpieces and quartz windows were used in a four-hole An-F rotor. A_{280} scans were performed after equilibrium was attained, usually between 24 and 36 h for 3-mm column heights. The molecular weight of AADH was determined by nonlinear least-squares analysis (21) in terms of equation 1:

$$c_r = B + c_m \exp[M(1 - v\rho)\omega^2(r^2 - r_m^2)/2RT] \quad (1)$$

where c_r is the concentration of the enzyme at a given radial position, c_m is the concentration of the enzyme at some reference position, for example, at the meniscus, M is the molecular weight, v is the partial specific volume, ρ is the solvent density, ω is the angular velocity, r is the radial position

TABLE 1. Purification of aromatic amine dehydrogenase

Purification step	Total protein (mg)	Total activity (U)	Specific activity (U/mg)	Purification factor	Yield (%)
Cell extract	3,925	1,523	0.39		100
Ammonium sulfate fractionation	2,880	1,228	0.43	1.1	81
DEAE chromatography	154	1,064	6.9	17.7	70
AcA 34 chromatography	46	658	14.3	36.7	43

in centimeters from the center of rotation, r_m is the distance in centimeters from the center of rotation to the meniscus, R is the gas constant, T is the absolute temperature in kelvins, and B is a correction term for a nonzero baseline. A partial specific volume of 0.73 ml/g was assumed, and solvent density was determined pycnometrically. Data for two different loading concentrations were analyzed simultaneously as a test for homogeneity (35) and to constrain confidence intervals for the parameter values (21).

(ix) Sequencing procedure. Polypeptides of AADH were prepared for sequencing by a modification of previously described protocols (28, 29). SDS-PAGE was prepared according to Laemmli (23), except that the stacking gel was omitted and wells were formed in the separating gel. After equilibration at room temperature for 12 h, the gels were prerun with Laemmli standard running buffer with the addition of 0.1 mM thioglycolate. AADH (20 μg) was loaded into each well, and electrophoresis was performed with fresh buffer. Prior to transfer onto an Immobilon-P (Millipore) polyvinylidene difluoride membrane, the gels were incubated for 15 min in the transfer buffer, which contained 12 mM Tris, 96 mM glycine, 10% methanol, and 0.5 mM dithiothreitol. Transfer of the polypeptides onto a membrane was performed with a wet transfer apparatus (Bio-Rad) at 100 V at 5°C for at least 12 h. This procedure resulted in transfer of approximately 50% of the large subunit and 100% of the small subunit. Glycine was removed from the membranes by washing with distilled water. The bands corresponding to the two subunits of AADH were cut out of the membrane, dried, and sequenced in an AB1476A protein sequencer (Applied Biosystems) at the microchemical facility at the California Institute of Technology. Since it was determined that the N terminus of the large subunit was blocked, sequencing was also performed on 100 μg of the holoenzyme bound by filtration directly onto an Immobilon-P membrane.

(x) Hybridization studies. The chromosomal DNA of *A. faecalis* was isolated according to the procedure of Marmur and Doty (24) and digested with *Bam*HI, *Pst*I, *Hin*dIII, and *Bst*YI. The resulting digests were analyzed by electrophoresis on a 0.7% agarose gel. The probe used for hybridization was a DNA fragment from the plasmid pAYC152.1 (6) that contains the *mauA* gene, which encodes the MADH small subunit, and a portion of the *mauD* gene of *Methylobacterium extorquens* AM1. The probe was labeled with a random-primed labeling kit as suggested by the manufacturer (Boehringer Mannheim). The hybridization was performed in dried gels at 45°C (27), and washing was done at the same temperature in 0.5× SSC (1× SSC is 0.15 M NaCl in 0.015 M sodium citrate) and 0.1% SDS. A *Bam*HI digest of chromosomal DNA from *M. extorquens* AM1 was used as a positive control.

RESULTS

Purification of AADH. The purification reported here (Table 1) is simpler than that which was reported previously (20, 32). The previous protocol also included chromatography steps over Bio-Gel A 15m and hydroxyapatite and a final crystallization step, which have been omitted. The procedure reported here results in a comparable yield of enzyme with a significantly higher specific activity than that previously reported (9.11 μmol/min/mg of protein) (20).

Subunit molecular weights. It is important to examine the subunit molecular weights of AADH in detail because of large discrepancies between the previously reported subunit molecular weights and those obtained in this study. AADH was analyzed by SDS-PAGE and exhibited two distinct bands which correspond in molecular weight to 39,000 and 18,000 (Fig. 2). The smaller band reacted positively in the redox cycling stain of Paz et al. (34), which indicated the presence of a covalently bound quinone on this subunit (data not shown). AADH was previously reported to possess subunits of molecular weight of 46,000 and 8,000 (20). The validity of our molecular weights is supported by comparing AADH with a sample of MADH from *P. denitrificans* (17), which has subunit molecular weights of 46,700 and 15,500 (Fig. 2). It is evident that AADH possesses a significantly smaller large subunit and larger small subunit than does MADH. Certain preparations of AADH exhibited two bands in the lower molecular weight range which correspond to 18,000 and 16,000. The second lower-molecular-weight species also appeared on aging of the purified enzyme and is probably the result of degradation of the smaller subunit.

FIG. 2. SDS-PAGE of AADH. The left lane contains Bio-Rad prestained molecular weight markers: phosphorylase *b*, 106,000; bovine serum albumin, 80,000; ovalbumin, 45,500; carbonic anhydrase, 32,500; soybean trypsin inhibitor, 27,500; lysozyme, 18,500. The center lane contains purified AADH. The right lane contains purified MADH from *P. denitrificans*.

Native molecular weight. The holoenzyme molecular weight of AADH was investigated by sedimentation equilibrium, with typical results for two initial protein concentrations run simultaneously, presented in Fig. 3A. These data, in terms of absorbance versus radius, were analyzed on the assumption of a single homogeneous species with equation 1, which yielded a molecular weight of approximately 108,900, with a 65% confidence interval of 108,100 to 109,700. As can be seen in Fig. 3B, the distribution of the residual errors (A_{280} observed $- A_{280}$ theoretical) is small and random, indicating an excellent fit of this simple model to the data. This molecular weight for the holoenzyme is in good agreement with the value of 114,000 estimated from the subunit molecular weights by SDS-PAGE on the assumption of an $\alpha_2\beta_2$ structure.

Immunochemical analysis. The degree of immunological cross-reactivity of the individual subunits of AADH with the corresponding subunits of MADH was ascertained by Western blotting. No cross-reactivity of AADH with antibodies which had been raised to the isolated subunits of *P. denitrificans* MADH was detected.

Isoelectric point. The isoelectric point of the enzyme was found to be 5.2, as determined by analysis on an isoelectric focusing gel.

Enzyme stability. The stability of AADH as a function of temperature was measured by incubating the purified enzyme (1 mg/ml in 50 mM potassium phosphate, pH 6.9) at temperatures ranging from 20 to 100°C for 20 min and then testing for enzyme activity. Full activity was retained up to 60°C. Above

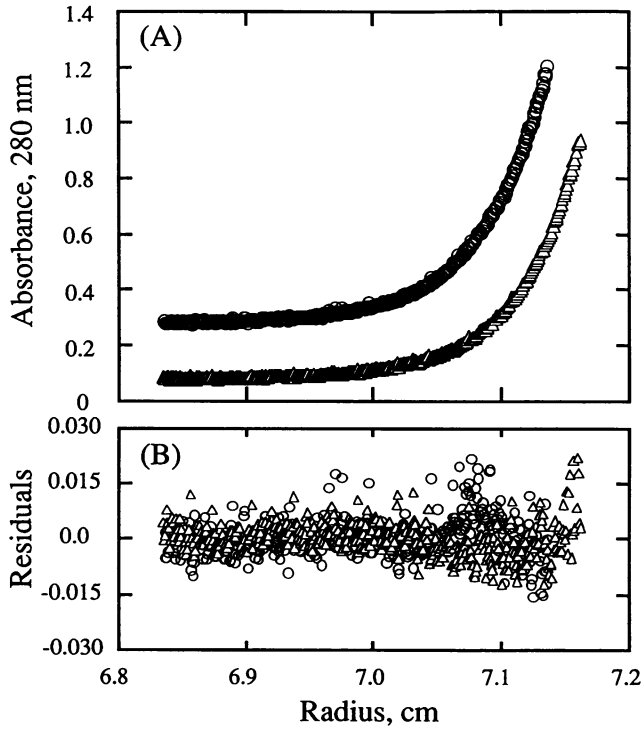

FIG. 3. Sedimentation equilibrium of AADH. Data in the form of A_{280} versus radial distance from the center of rotation were collected after 31 h as described in Materials and Methods. (A) Primary data obtained at two different initial loading concentrations, 0.25 mg/ml (triangles) and 0.5 mg/ml (circles), were used to test for homogeneity. The rotor speed was 15,026 rpm and the temperature was 21°C. (B) Residual error versus radial distance from the center of rotation for simultaneous analysis of both concentrations in terms of a single, homogeneous species as described in equation 1.

80°C, the activity dropped to less than 10%. In addition, it was noted that the small subunit of the enzyme remained in solution after heating at 100°C for 5 min, while the large subunit precipitated.

AADH was also quite stable against denaturation by guanidine hydrochloride. Protein samples were incubated with guanidine hydrochloride for 30 min at 22°C in 50 mM phosphate buffer, pH 7.0. Full enzyme activity was retained in the presence of concentrations of guanidine hydrochloride up to 2 M. Activity fell to less than 20% at concentrations greater than 4 M.

Reconstitution of subunits. The subunits of AADH were separated as described in Materials and Methods. SDS-PAGE analysis of the isolated subunits showed bands which correspond to those of the native enzyme. The subunits were reconstituted by mixing a stoichiometric amount of the large and small subunits in 1.8 M potassium phosphate buffer, pH 7.0, at 30°C. After 30 min, enzyme activity was assayed. For control purposes, the individual subunits were also assayed under the same conditions. The large and small subunits incubated alone did not show any activity, whereas the mixture of the two exhibited 42% of the native enzyme activity.

Partial amino acid sequence. Three attempts to obtain the N-terminal sequence for the large subunit from two different preparations of AADH were made. No amino acids were recovered after three cycles of sequencing, indicating that the N terminus was blocked. The N-terminal amino acid sequence for the small subunit polypeptide was determined in two separate experiments: after transfer of the dissociated large and small subunits onto a polyvinylidene difluoride membrane (separated by SDS-PAGE) and after adsorption of the AADH holoenzyme onto a polyvinylidene difluoride membrane. Both experiments gave the same sequence: Ala-Gly-Gly-Gly-Gly-Ser-Ser-Ser-Gly-Ala-Asp-His-Ile-Ile-Leu-(Asn)-(Pro). This N-terminal amino acid sequence of AADH exhibits no homology at all with the known sequences of the N termini of known small subunits of MADHs (9, 19).

Hybridization studies. The absence of substantial sequence homology between the small subunits of MADH and AADH was corroborated by hybridization experiments in which digests of the *A. faecalis* chromosome were hybridized with a DNA fragment carrying the *mauA* gene, which codes for the small subunit of MADH from *M. extorquens* AM1 (6), as a probe. No hybridization between the probe and *A. faecalis* DNA was observed, whereas a high level of hybridization between the probe and *M. extorquens* AM1 DNA in control experiments was observed (data not shown).

Absorption spectra. The visible absorption spectrum of the fully oxidized form of AADH exhibited a peak centered at 456 nm and significant absorbance between 500 and 800 nm. Titration of this enzyme with tyramine proceeded directly from the fully oxidized to the fully reduced species (Fig. 4). Addition of substoichiometric amounts of tyramine to AADH caused a reduction of A_{456}, an increase in A_{327}, and a progressive reduction of absorbance beyond 500 nm. An isosbestic point was maintained at 365 nm, and absorbance changes were linear throughout the titration (Fig. 4). The maximum change in absorbance caused by the addition of each increment of tyramine occurred very rapidly. The fully reduced form of AADH was somewhat susceptible to reoxidation under aerobic conditions. Approximately 50% reoxidation of the tyramine-reduced enzyme was observed after 3 h, and complete reoxidation occurred after 20 h. A quantitative anaerobic titration of AADH with tyramine yielded an extinction coefficient (Table 2) which is significantly higher than that which was previously reported (20, 32). This may be explained by the susceptibility of reduced AADH to oxidation. If the reductive titration is not performed under strict anaerobic conditions, some reoxidation will occur and an excess of a stoichiometric amount of tyramine will be required to achieve full reduction of the enzyme. This would result in an underestimation of the experimentally determined extinction coefficient. The complete anaerobic titration of AADH consumed 2.1 mol of tyramine per mol of enzyme. These data are consistent with the presence of 2 mol of TTQ per mol of enzyme.

Whereas the titration of AADH with tyramine proceeded directly from the oxidized quinone to reduced quinol, the semiquinone could be generated by addition of one molar equivalent of dithionite per quinone prosthetic group (Fig. 5). The transition from the fully oxidized enzyme to the semiquinone was characterized by a significant increase in absorbance of the major peak and concomitant shift to an absorbance maximum at 433 nm (Fig. 5). Addition of a second molar equivalent of dithionite resulted in formation of the fully reduced enzyme. The final spectrum obtained from the tyramine titration was very similar to that obtained in the dithionite titration except that the absorption maximum for the dithionite-reduced enzyme was at 332 nm compared with 327 nm in substrate-reduced AADH.

As stated above, reduced AADH was somewhat susceptible to reoxidation by air. Complete reoxidation of the reduced enzyme could be achieved within a few hours by addition of ferricyanide. An oxidative titration of the reduced enzyme with

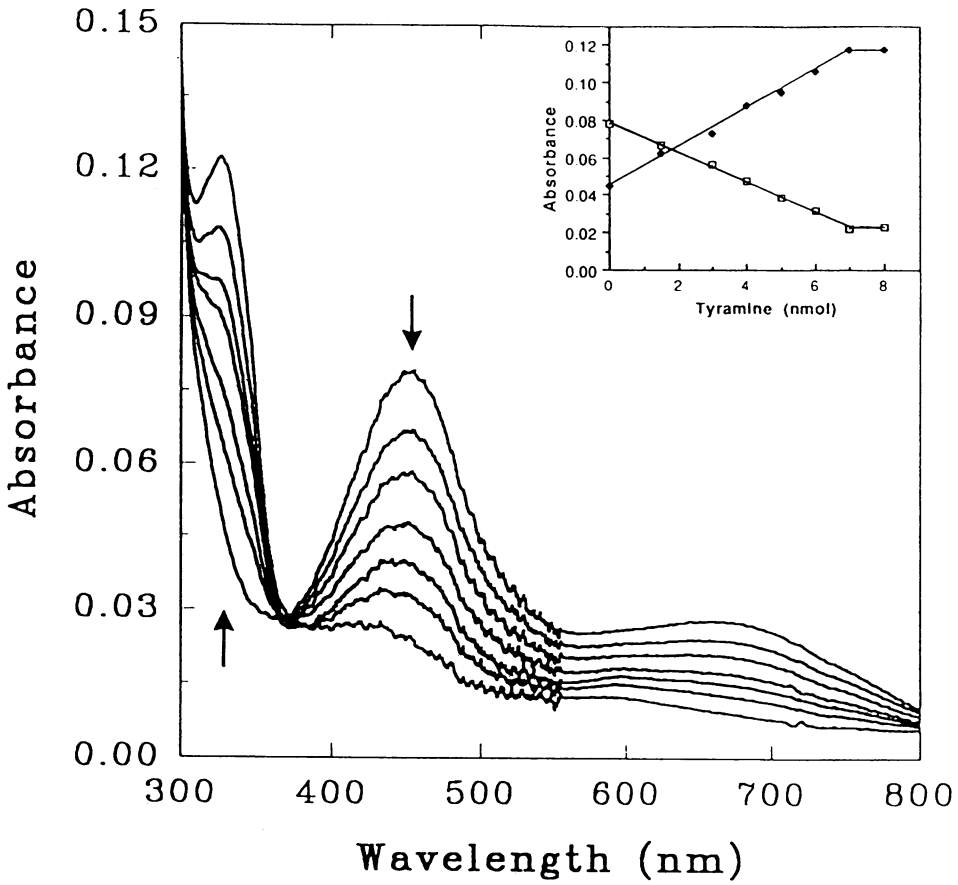

FIG. 4. Substrate titration of oxidized AADH. AADH (3.3 nmol) in 50 mM potassium phosphate, pH 7.5, was deoxygenated and titrated with an anaerobic solution of tyramine HCl at 20°C. Spectra were recorded 3 min after addition of 0 (curve 1), 1.5 (curve 2), 3.0 (curve 3), 4.0 (curve 4), 5.0 (curve 5), 6.0 (curve 6), and 7 nmol (curve 7) of tyramine HCl. The direction of the spectral changes on addition of tyramine are indicated with curve 1 nearest the arrows. The changes in A_{327} (closed symbols) and A_{456} (open symbols) which were observed during the titration are summarized in the inset.

ferricyanide gave results which were consistent with those observed in the reductive titration of the oxidized enzyme with tyramine. The molar extinction coefficients, calculated from the data obtained during these titrations, at selected wavelengths for each of the three redox states of the enzyme are given in Table 2. Comparison with the values for *P. denitrificans* MADH (Table 2) shows that there are strong spectral similarities for all three redox forms. These results indicate that AADH also contains the TTQ cofactor.

Resonance Raman spectra. Excitation of AADH at its 456-nm absorption maximum led to a resonance Raman spectrum with a large number of vibrational modes between 900 and 1,700 cm^{-1} (Fig. 6B). The frequencies and intensities were remarkably similar to those reported previously for MADH (Fig. 6A). Both proteins exhibited intense peaks at approximately 1,001, 1,065, 1,165, 1,454, 1,570, 1,580, and 1,625 cm^{-1}. These results provide definitive identification of a TTQ cofactor in AADH. In MADH, the peak at 1,625 cm^{-1} was assigned to the in-phase symmetric stretch of the two quinone C=O groups on the basis of its ^{18}O dependence (1, 25). The unusually low frequency of this mode compared with the typical quinone value of about 1,675 cm^{-1} was believed to be due to strong hydrogen bonding of one or both of the cofactor oxygens (1). A similar degree of hydrogen bonding of the C=O groups is likely to be present in AADH.

TABLE 2. Absorption properties of AADH and MADH

Enzyme	Redox state	Extinction coefficient (mM^{-1} cm^{-1})[a] at:				
		330 nm	428 nm	433 nm	440 nm	456 nm
AADH	Oxidized	13.5		27.6		31.6
	Semiquinone	25.7		41.1		19.5
	Reduced	47.8		4.6		3.6
MADH[b]	Oxidized	20.6	25.2		26.2	
	Semiquinone	25.2	50.4		11.2	
	Reduced	56.4	1.8		1.2	

[a] One mole of enzyme refers to the holoenzyme which contains 2 mol of TTQ.
[b] Data for *P. denitrificans* MADH are taken from reference 18.

Steady-state kinetics. The enzyme assay is based on the procedure described originally by Eady and Large (14) for MADH. The immediate electron acceptor for reduced AADH is phenazine ethosulfate or phenazine methosulfate, which is then reoxidized by 2,6-dichlorophenol-indophenol (DCIP). Reduction of DCIP is easily monitored by a decrease in its A_{600}. The physiologic electron receptor for AADH is not yet known.

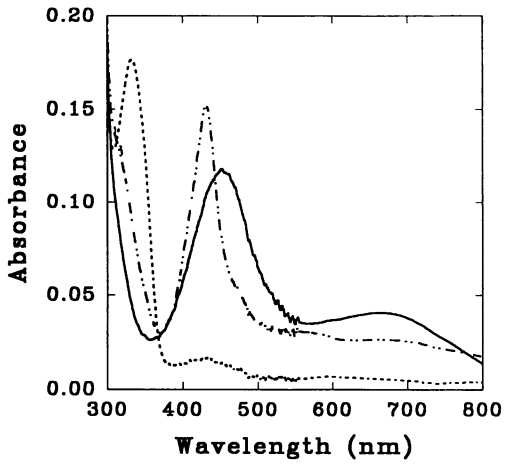

FIG. 5. Formation of the semiquinone and reduced forms of AADH on addition of dithionite. Spectra were recorded of AADH (3.8 μM) in 50 mM potassium phosphate, pH 7.5, before (——) and after addition of one molar equivalent of sodium dithionite (—··—) and a second molar equivalent of sodium dithionite (– – – –).

At high substrate concentrations, substrate inhibition of AADH was observed. Data were fit, therefore, to equation 2.

$$v_o = \frac{V_{max}(S)}{K_m + (S) + (S)^2/K_i} \quad (2)$$

where v_o is the initial reaction rate, (S) is the substrate concentration, and V_{max} is the maximum initial reaction velocity. A K_m value for tyramine of 5.4 μM and a V_{max} of 17 μmol/min/mg of protein were determined. The K_i value for substrate inhibition by tyramine was 1.08 mM. At saturating concentrations of tyramine, phenazine methosulfate and phenazine ethosulfate exhibited apparent K_m values of 0.25 and 0.45 mM, respectively.

Inhibition of AADH. Phenylhydrazine, hydroxylamine, and semicarbazide had been reported to inhibit the activity of AADH (20). This has been confirmed in the present study, and it has further been shown that the inhibition by these compounds, as well as by hydrazine and aminoguanidine, is due to an irreversible inactivation of AADH. These five carbonyl reagents have been shown previously to also irreversibly inactivate MADH (11). Two other compounds, isonicotinic acid hydrazide (isoniazid) and isonicotinic acid 2-isopropyl hydrazide (iproniazid), were also tested as possible inhibitors of AADH. Each of these compounds reversibly inhibited AADH. Steady-state kinetic analyses of the inhibition by isoniazid and iproniazid indicated that the inhibition was noncompetitive. Isoniazid exhibited a K_i of 8.4 μM, and iproniazid exhibited a K_i of 186 μM. Addition of isoniazid and iproniazid to AADH also caused changes in the absorption spectrum of AADH characterized by a shift of the visible absorption maximum from 456 to 407 nm.

DISCUSSION

This paper presents a simplified procedure for the purification of AADH, corrects the previously reported erroneous subunit molecular weights and extinction coefficient of AADH, and describes in detail certain kinetic and spectral properties of this enzyme. The resonance Raman spectrum provides definitive evidence that AADH possesses the same TTQ

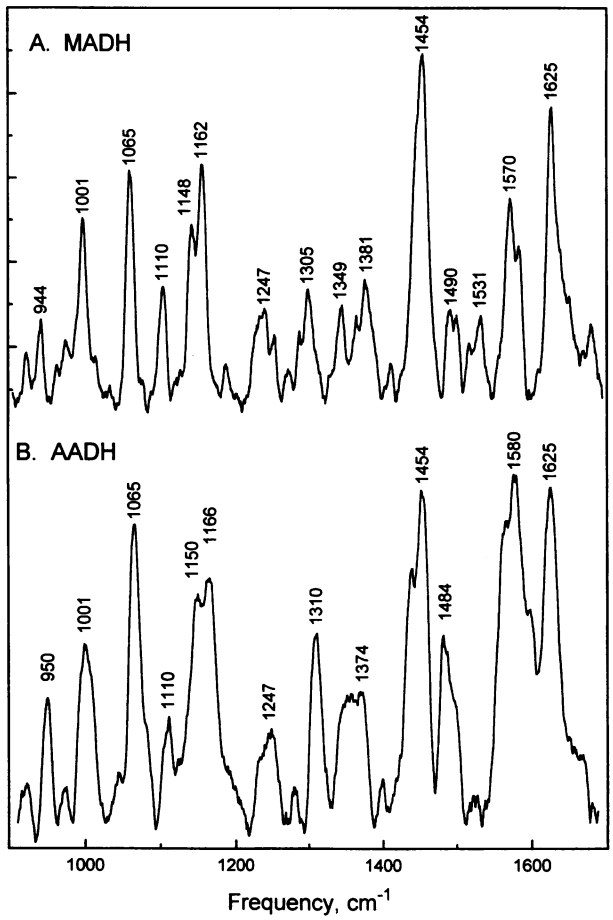

FIG. 6. Resonance Raman spectra of MADH and AADH obtained with 457.9-nm excitation. (A) *P. denitrificans* MADH (0.6 mM) in 0.01 M phosphate (pH 7.5). Spectral conditions: 70 mW laser power, 1 cm^{-1}/s scan rate, 5 cm^{-1} resolution, and 16 scans. (B) AADH (0.2 mM) in 0.05 M Tris-HCl (pH 7.4). Spectral conditions: 30 mW laser power, 1 cm^{-1}/s scan rate, 6 cm^{-1} resolution, and 16 scans.

prosthetic group as MADH. This has been further verified by observing closely similar resonance Raman spectral patterns for the hydroxylamine adducts of AADH and MADH (7). In view of the presence of the same cofactor in both enzymes, special attention has been given to a comparison of their physical and kinetic properties.

The subunit molecular weights of AADH are similar to, but distinctly different from, those reported for the quinoprotein MADH. The weight of the large subunit is smaller than that of the corresponding subunit of any MADH, and the weight of the small subunit is larger than that of the corresponding subunit of any MADH. The small subunit of AADH stains positively in the redox cycling assay for covalently bound quinones, as does the small subunit of MADH. The small subunits of MADHs from diverse bacterial sources are highly conserved and exhibit strong sequence homology (9) and immunological cross-reactivity (12). Despite possessing the identical TTQ cofactor, the small subunit of AADH does not cross-react immunologically with that subunit of MADH and exhibits an N-terminal amino acid sequence which bears no resemblance to any of the three MADHs which have been sequenced. It is interesting to note that like AADH, MADHs

from *P. denitrificans* (10) and *Thiobacillus versutus* (38) also possess a blocked N terminus of the large subunit.

The visible absorption spectra of the three redox states of AADH are very similar to those exhibited by MADH (18) and are quite consistent with the presence of the same prosthetic group in each enzyme. Certain similarities are particularly noteworthy. In both enzymes, no semiquinone was observed during a reductive titration with substrate, but titration with dithionite proceeded through the semiquinone. This indicates that in each there is a kinetic barrier to the transfer of the second electron to TTQ. The reduced and semiquinone forms of both enzymes are relatively stable towards reoxidation under aerobic conditions. Therefore, the protein environment of TTQ is somehow helping to stabilize the reduced and semiquinone species which would otherwise be highly unstable in solution. The reduced AADH was, however, somewhat susceptible to reoxidation, in contrast to MADH, which was very resistant to reoxidation (18). Eventual elucidation of the structures of each of these enzymes may provide insight as to what accounts for this stabilization of otherwise unstable redox forms of the cofactor.

AADH and MADH are also each remarkably stable against denaturation. Both AADH and MADH (17, 36) exhibit considerable thermal stability and resistance to denaturation by guanidine hydrochloride. The thermal stability of the small subunit of AADH was found to be greater than that of the large subunit. After 5 min of boiling, the large subunit precipitated while the small subunit remained in solution with the cofactor still attached. This result is in agreement with the likely covalent attachment between cofactor and peptide in AADH as has been demonstrated in MADH. The isolated subunits of AADH could also be at least partially reconstituted to form active enzyme. Similar reconstitution has been demonstrated for MADHs (12, 36).

AADH was irreversibly inactivated by carbonyl reagents, such as phenylhydrazine. These compounds have previously been shown to be irreversible inhibitors of other amine-oxidizing enzymes, such as the flavoprotein monoamine oxidase and the quinoprotein MADH. With the flavoproteins, inhibition appears to be mechanism based and involves formation of a free radical intermediate which forms a covalent adduct with the cofactor (22, 33). With MADH, inactivation occurred by direct reaction with TTQ and apparent formation of a hydrazone adduct (11). AADH was also inhibited by iproniazid, another monoamine oxidase inhibitor. Monoamine oxidase is irreversibly inactivated by iproniazid by a mechanism which is not clear but may first involve conversion of iproniazid to isopropylhydrazine (37). In contrast, inhibition of AADH was reversible and apparently noncompetitive. Similar inhibition with a structurally similar compound, the antitubercular drug isoniazid, was observed. Isoniazid and iproniazid caused perturbation of the absorption spectrum, indicating that the binding of these inhibitors affects the cofactor or its environment. Although these inhibitors have structures similar to that of tyramine, enzyme kinetic measurements suggest that they are noncompetitive inhibitors and perhaps may not bind at the substrate binding site. The basis for the similarities in the mechanism of inhibition of AADH and monoamine oxidase by these compounds remains to be elucidated and may provide information on the general mechanism of the oxidation of biogenic amines by these diverse enzymes.

MADHs from two bacterial sources have been crystallized. The structure of MADH from *T. versutus* has been solved at 2.25 Å (0.225 nm) (39), and MADH from *P. denitrificans* has been solved at 2.8 Å (0.2.8 nm) (4). AADH from *A. faecalis* has also recently been crystallized (16). Detailed resonance Raman spectra have been obtained for AADH (7) and for MADHs from *T. versutus*, *P. denitrificans*, and bacterium W3A1 (1, 25); these data indicated that each of these three enzymes possessed the identical cofactor. Together with the structural information, this characterization of the similarities and differences in the physical and kinetic properties of AADH and MADH will provide a basis for understanding what specific aspects of the protein structure endow the protein-bound TTQ with its particular properties. Further biochemical studies in conjunction with structural and biophysical studies of AADH and MADH will provide a detailed picture of the fascinating TTQ prosthetic group and, it is hoped, will provide insight into why nature has chosen to include TTQ among its wide array of cofactors, many of which would also be capable of catalyzing amine oxidation reactions.

ACKNOWLEDGMENTS

This research was supported by NIH grants GM41574 (V.L.D.) and GM34468 (J.S.-L.) and NSF grants DMB87-16316 (S.G.) and DMB90-02177 (E.E.).

We thank Gabriele Backes for assistance in obtaining resonance Raman spectra.

REFERENCES

1. **Backes, G., V. L. Davidson, F. Huitema, J. A. Duine, and J. Sanders-Loehr.** 1991. Characterization of the tryptophan-derived quinone cofactor of methylamine dehydrogenase by resonance Raman spectroscopy. Biochemistry **30:**9201–9210.
2. **Bradford, M. M.** 1976. A rapid and simple method for the quantitation of microgram quantities of protein utilizing the principle of protein-dye binding. Anal. Biochem. **72:**248–254.
3. **Chen, L., F. S. Mathews, V. L. Davidson, E. Huizinga, F. M. D. Vellieux, J. A. Duine, and W. G. J. Hol.** 1991. Crystallographic investigations of the tryptophan-derived cofactor in quinoprotein methylamine dehydrogenase. FEBS Lett. **287:**163–166.
4. **Chen, L., F. S. Mathews, V. L. Davidson, E. Huizinga, F. M. D. Vellieux, and W. G. J. Hol.** 1992. Three-dimensional structure of quinoprotein methylamine dehydrogenase from *Paracoccus denitrificans* determined by molecular replacement at 2.8 Å., Proteins Struct. Funct. Genet. **14:**288–299.
5. **Chistoserdov, A. Y., Y. D. Tsygankov, and M. E. Lidstrom.** 1990. Cloning and sequencing of the structural gene for the small subunit of MADH from *Methylobacterium extorquens* AM1: evidence for two tryptophan residues involved in the active center. Biochem. Biophys. Res. Commun. **172:**211–216.
6. **Chistoserdov, A. Y., Y. D. Tsygankov, and M. E. Lidstrom.** 1991. Genetic organization of methylamine utilization genes from *Methylobacterium extorquens* AM1 J. Bacteriol. **173:**5901–5908.
7. **Cohen, J., G. Backes, and J. Sanders-Loehr.** 1993. Personal communication.
8. **Davidson, V. L.** 1990. Methylamine dehydrogenases from methylotrophic bacteria. Methods Enzymol. **188:**241–246.
9. **Davidson, V. L.** 1993. Methylamine dehydrogenase, p. 73–95. *In* V. L. Davidson (ed.), Principles and applications of quinoproteins. Marcel Dekker, New York.
10. **Davidson, V. L., unpublished data.**
11. **Davidson, V. L., and L. H. Jones.** 1992. Cofactor-directed inactivation by nucleophilic amines of the quinoprotein methylamine dehydrogenase from *Paracoccus denitrificans*. Biochim. Biophys. Acta **1121:**104–110.
12. **Davidson, V. L., and J. W. Neher.** 1987. Evidence for two subclasses of methylamine dehydrogenases with distinct large subunits and conserved PQQ-bearing small subunits. FEMS Microbiol. Lett. **44:**121–12.
13. **De Beer, R., J. A. Duine, J. Frank, Jzn., and P. J. Large.** 1980. The prosthetic group of methylamine dehydrogenase from *Pseudomonas* AM1. Biochim. Biophys. Acta **622:**370–374.
14. **Eady, R. R., and P. J. Large.** 1968. Purification and properties of an amine dehydrogenase from *Pseudomonas* AM1 and its role in

growth on methylamine. Biochem. J. **106:**245–255.
15. **Eady, R. R., and P. J. Large.** 1971. Microbial oxidation of amines. Spectral and kinetic properties of the primary amine dehydrogenase of *Pseudomonas* AM1. Biochem. J. **123:**757–768.
16. **Edwards, S. L.** Unpublished data.
17. **Husain, M., and V. L. Davidson.** 1987. Purification and properties of methylamine dehydrogenase from *Paracoccus denitrificans*. J. Bacteriol. **169:**1712–1717.
18. **Husain, M., V. L. Davidson, K. A. Gray, and D. B. Knaff.** 1987. Redox properties of the quinoprotein methylamine dehydrogenase from *Paracoccus denitrificans*. Biochemistry **26:**4139–4143.
19. **Ishii, Y., T. Hase, Y. Fukumori, H. Matsubara, and J. Tobari.** 1983. Amino acid sequence studies of the light subunit of methylamine dehydrogenase from *Pseudomonas* AM1: existence of two residues binding the prosthetic group. J. Biochem. **93:**107–119.
20. **Iwaki, M., T. Yagi, K. Horiike, Y. Saeki, T. Ushijima, and M. Nozaki.** 1983. Crystallization and properties of aromatic amine dehydrogenase from *Pseudomonas* sp. Arch. Biochem. Biophys. **220:**253–262.
21. **Johnson, M. L., and S. G. Fraser.** 1985. Nonlinear least-squares analysis. Methods Enzymol. **117:**301–342.
22. **Kenny, W. C., J. Nagy, J. I. Salach, and T. P. Singer.** 1979. Structure of the covalent phenylhydrazine adduct of monoamine oxidase, p. 25–37. *In* T. P. Singer, R. W. von Korff, and D. L. Murphy (ed.), Monoamine oxidase: structure, function, and altered functions. Academic Press, New York.
23. **Laemmli, U. K.** 1970. Cleavage of structural proteins during the assembly of the head of bacteriophage T4. Nature (London) **227:**680–685.
24. **Marmur, J., and P. Doty.** 1962. Determination of the base composition of deoxyribonucleic acid from its thermal denaturation temperature. J. Mol. Biol. **5:**109–113.
25. **McIntire, W. S., J. L. Bates, D. E. Brown, and D. M. Dooley.** 1991. Resonance Raman spectroscopy of methylamine dehydrogenase from bacterium W3A1. Biochemistry **30:**125–133.
26. **McIntire, W. S., D. E. Wemmer, A. Y. Chistoserdov, and M. E. Lidstrom.** 1991. A new cofactor in a prokaryotic enzyme: tryptophan tryptophylquinone as the redox prosthetic group in methylamine dehydrogenase. Science **252:**817–824.
27. **Meinkoth, J. B. M., and G. Wahl.** 1984. Hybridization of nucleic acids immobilized on a solid support. Anal. Biochem. **138:**267–284.
28. **Moos, M., N. Y. Nguyen, and T.-Y. Liu.** 1988. Reproductive high yield sequencing of proteins electrophoretically separated and transferred to an inert support. J. Biol. Chem. **263:**6005–6008.
29. **Mozdzanowsky, J., P. Hembach, and D. W. Speicher.** 1992. High yield electroblotting onto polyvinylidene difluoride membranes from polyacrylamide gels. Electrophoresis **13:**59–64.
30. **Murooka, Y., N. Doi, and T. Harada.** 1979. Distribution of membrane-bound monoamine oxidase in bacteria. Appl. Environ. Microbiol. **38:**565–569.
31. **Nichols, R., C. D. Weaver, E. Eisenstein, R. L. Blakely, J. Appleman, T.-H. Huang, F.-Y. Huang, and E. E. Howell.** 1993. Titration of histidine 62 in R67 dihydrofolate reductase is linked to a tetramer-two dimer equilibrium. Biochemistry **32:**1695–1706.
32. **Nozaki, M.** 1987. Aromatic amine dehydrogenase from *Alcaligenes faecalis*. Methods Enzymol. **142:**650–655.
33. **Patek, D. R., and L. Hellerman.** 1974. Mitochondrial monoamine oxidase. J. Biol. Chem. **249:**2373–2380.
34. **Paz, M. A., R. Fluckiger, A. Boak, H. M. Kagan, and P. M. Gallop.** 1991. Specific detection of quinoproteins by redox-cycling staining. J. Biol. Chem. **266:**689–692.
35. **Roark, D. E.** 1976. Sedimentation equilibrium techniques: multiple speed analyses and an overspeed procedure. Biophys. Chem. **5:**185–196.
36. **Shirai, S., T. Matsumoto, and J. Tobari.** 1978. Methylamine dehydrogenase of *Pseudomonas* AM1. A subunit enzyme. J. Biochem. **83:**1599–1607.
37. **Smith, T. E., H. Weissbach, and S. Underfriend.** 1963. Studies on monoamine oxidase: the mechanism of inhibition of monoamine oxidase by iproniazid. Biochemistry **2:**746–751.
38. **van Beeumen, J., G. van Driessche, F. Huitema, J. A. Duine, and G. W. Canters.** 1993. N-terminal heterogeneity of methylamine dehydrogenase from *Thiobacillus versutus*. FEBS Lett. **333:**188–192.
39. **Vellieux, F. M. D., F. Huitema, H. Groendijk, K. H. Kalk, J. Frank, J. A. Jongejan, J. A. Duine, K. Petratos, J. Drenth, and W. G. J. Hol.** 1989. Structure of quinoprotein methylamine dehydrogenase at 2.25 Å resolution. EMBO. J. **8:**2171–2178.